HAYATI
Journal of Biosciences

Vol. 31 No. 5, September 2024 951-963
DOI:10.4308/hjb.31.5.951-963
ISSN: 1978-3019
EISSN: 2086-4094

The *In Vitro* and *In Silico* Study of α-glucosidase Inhibition by Kombucha Derived from *Syzygium polyanthum* (Wight) Walp. Leaves

Sitaresmi Yuningtyas[1*], Muhammad Alfarabi[2], Yunita Lestari[1], Harry Noviardi[1]

[1]*Department of Pharmacy, Sekolah Tinggi Teknologi Industri dan Farmasi Bogor, Bogor 16128, Indonesia*
[2]*Department of Biochemistry, Faculty of Medicine, Universitas Kristen Indonesia, East Jakarta 13630, Indonesia*

ARTICLE INFO

Article history:
Received October 22, 2023
Received in revised form March 2, 2024
Accepted April 25, 2024

KEYWORDS:
α-glucosidase,
diabetes mellitus,
enzyme inhibitor,
fermentation,
kombucha,
Syzygium polyanthum

ABSTRACT

Kombucha is a fermented tea drink using a symbiotic culture of bacteria and yeast. This drink has been widely used to maintain blood sugar levels. Meanwhile, leaf boiled water of *Syzygium polyanthum* (Wight) Walp. has been used as an alternative medicine for diabetes mellitus in Indonesia. If this herb is made into kombucha, it may have higher antihyperglycemic activity than kombucha from tea leaves. However, there are no scientific reports of antihyperglycemic activity from *S. polyanthum* leaf kombucha by inhibiting alpha-glucosidase. This study aims to determine the activity and kinetics inhibition of *S. polyanthum* leaves kombucha against α-glucosidase. Samples were prepared at varying concentrations (12.5, 25, 37.5, 50 g/L), while phytochemical components in the products were identified, and the inhibitory activity as well as kinetics were comprehensively analyzed. *In silico* evaluations were conducted to further explore the inhibitory activity. The results showed that the products contained secondary metabolites such as flavonoids, saponins, and tannins. The inhibitory activity against α-glucosidase ranged from 81.05 to 89.41%. The inhibition mechanism was identified as uncompetitive, with a Michaelis-Menten constant (K_M) of 0.1357 mM and a v_{max} value of 27.7008 U/ml minute. Several metabolites showed promising inhibition potential due to their strong binding interactions with α-glucosidase, including hydrogen bonding (H-bond), hydrophobic interactions, van der Waals forces, and electrostatic forces. Additionally, two metabolites, farnesol and α-pinene, were found to interact with other human proteins. These observations showed the potential of *S. polyanthum* leaves kombucha as a health-promoting beverage that might aid blood sugar control in diabetic individuals.

1. Introduction

Diabetes mellitus (DM) is a predominant degenerative disease affecting a significant portion of the population. The International Diabetes Federation predicts a rise in DM cases in Indonesia, from 10.7 million in 2019 to 13.7 million by 2030. National Health Survey (Riskesdas) in 2018 showed a diagnosed DM prevalence of 2% among individuals aged 15 and above, compared to the 1.5% documented in 2013. The highest prevalence is observed within the age groups of 55-64 and 65-74 years (Kementerian Kesehatan Republik Indonesia 2020). In managing DM, chemical or natural remedies derived from plants or animals can be used. Specifically, Indonesian society prefers natural remedies due to being considered more accessible, safer, and suitable for consumption, generally in the form of traditional herbal medicine or functional foods. Consequently, the exploration of natural resources for their potential as medicinal and functional food ingredients is necessary.

Natural resources with a potential medicinal application include *S. polyanthum* (Wight) Walp. leaves, which exhibit pharmacological properties such as antioxidant, antidiabetic, antihypertensive, antibacterial, antifungal, antidiarrheal, anti-cancer, antitumor, anti-plaque, anti-hyperlipidemia, and acetylcholinesterase inhibition activities (Ismail and Ahmad 2019). Their use as a traditional remedy is

* Corresponding Author
E-mail Address: sitaresmi.yuningtyas@gmail.com

based on the presence of various active components or metabolites, comprising phenolic compounds, organic acids, flavonoids, and terpenoids, that facilitate disease treatment (Rahim *et al.* 2018; Dewijanti *et al.* 2020; Widyawati *et al.* 2015, 2022; Rochmat *et al.* 2022; Syabana *et al.* 2022). For instance, *S. polyanthum* leaves have been found to possess antidiabetic potential. *In vivo* studies on this plant showed extract concentrations of 0.5-5.0 mg/kg, majorly containing phytol, capable of reducing blood glucose levels in Wistar rats over an 8-week administration period (Wahjuni *et al.* 2018).

Kombucha is a functional drink and produced from the fermentation of tea and sugar using a symbiotic culture of bacteria and yeast (SCOBY). The specific microorganism strains present in kombucha starter culture vary, influencing the characteristics of the fermentation product. Commonly, the bacteria used belong to the *Acetobacter* and *Gluconobacter* genera, while the yeast components include *Saccharomycodes* sp., *Saccharomyces* sp., *Zygosaccharomyces* sp., *Schizosaccharomyces* sp., *Candida* sp., *Torulospora* sp., *Brettanomyces* sp., *Pichia* sp., *Kloeckera* sp., *Mycoderma* sp., and *Mycotorula* sp. (Jayabalan *et al.* 2014). The symbiotic relationship between these microorganisms has been stated not to cause diseases, side effects, or toxicity (Laureys *et al.* 2020).

The transformation of tea into kombucha can lead to the formation of new metabolites or enhance the activity of metabolites beneficial for health. Additionally, the fermentation process often initiates alterations in the organic acid and polyphenol content. Kombucha comprises metabolites in the form of organic acids such as acetic acid, glucuronic acid, gluconic acid, and lactic acid (Leal *et al.* 2018; Yang *et al.* 2022). This beverage offers several health benefits, including digestion health, immune modulation, antimicrobial characteristics, prevention of heart disease and cancer, hypoglycemic and hyperlipidemic effects, and antioxidant properties (Dutta and Paul 2019).

Tea is known for being beneficial to health, and fermenting this resource into kombucha can further enhance its ability to promote well-being. Kombucha produced from *S. polyanthum* leaves (SPLK) contains secondary metabolites belonging to the flavonoid, saponin, tannin, and polyphenol groups. The antioxidant activity of this beverage exhibits an IC_{50} value of 27 g/L (Yuningtyas *et al.* 2021), but the antidiabetic potential and mechanisms of action are still unknown. Therefore, this study aimed to examine the activity and kinetics inhibition of SPLK against α-glucosidase, a key enzyme in regulating blood sugar levels among diabetic patients, and identify the phytochemical components. To enhance the understanding of the inhibition reaction between SPLK metabolites and α-glucosidase, a molecular docking analysis was conducted *in silico*.

2. Materials and Methods

2.1. Materials

Fresh leaves of *S. polyanthum* were collected from Balai Penelitian Tanaman Rempah and Obat (BALITRO) in Bogor, West Java, Indonesia. Additionally, SCOBY, containing *Acetobacter xylinum, Brettanomyces* sp., *Zygosaccharomyces* sp., and *Saccharomyces cerevisiae*, was obtained from Indokombucha, located in Bandung, West Java.

2.2. Methods

2.2.1. Production of SPLK

Dried *S. polyanthum* leaves simplicia were weighed and added to water to achieve concentrations of 12.5, 25, 37.5, and 50 g/L. The resulting mixture was boiled at 90°C for 15 minutes, then sugar (10% w/v) was introduced into the filtrate and cooled to 25°C. The filtrate was inoculated with SCOBY at a concentration of 100 g/L, and the container was covered using a cloth. Incubation was conducted at room temperature for eight days (Yuningtyas *et al.* 2021). SPLK generated was subjected to various analyses, including phytochemical screening, pH determination, α-glucosidase enzyme inhibition activity testing, and α-glucosidase kinetic determination.

2.2.2. Phytochemical Screening

The qualitative phytochemical screening of SPLK included detecting alkaloids, flavonoids, saponins, tannins, steroids, and terpenoids (Sivanandham 2015).

2.2.3. Alkaloid Test

Approximately 5 ml of SPLK was placed in a test tube, followed by the addition of 1 ml of 2 N hydrochloric acid and 10 ml of water. The mixture was heated in a water bath for 2 minutes, allowed to cool, and filtered. The resulting filtrate was divided into three separate test tubes, to which Mayer's,

Dragendorff's, and Wagner's reagents were added, respectively. The formation of white, red-orange, and brown precipitates in the first, second, and third tubes, respectively, showed the presence of alkaloids.

2.2.4. Flavonoid Test

A 5 ml of SPLK was heated for 5 minutes, filtered, and then magnesium powder, HCl: ethanol (1:1), and amyl alcohol were added to the filtrate. The formation of an orange to reddish-purple precipitate confirmed a positive result.

2.2.5. Saponin Test

Up to 5 ml of SPLK was vigorously shaken in a test tube, and the development of stable foam signified the presence of saponins.

2.2.6. Tannin Test

A 5 ml sample of SPLK was treated with 1% $FeCl_3$, and the appearance of a greenish-brown or bluish-black color showed the presence of tannins.

2.2.7. Terpenoid and Steroid Test

Approximately 5 ml of SPLK was evaporated in an evaporating dish and the resulting residue was dissolved in 0.5 ml of chloroform. Subsequently, 0.5 ml of acetic anhydride and 2 ml of concentrated sulfuric acid were added along the wall of the tube. The formation of brown or violet and bluish-green rings at the border of the solution suggested the presence of triterpenoids and steroids, respectively.

2.3. Inhibition of α-glucosidase

During the assay conducted, a total of 980 µL of 0.1 M pH 7 phosphate buffer, 500 µL of 20 mM pNPG (p-Nitrophenyl α-D-glucopyranoside), 20 µL of SPLK, and 500 µL of α-glucosidase enzyme were combined in a microplate. The mixture was incubated for 15 minutes at 37°C and the reaction was stopped by adding 2 ml of 200 mM Na_2CO_3. Furthermore, the absorbance was measured with a UV-Vis spectrophotometer (BioTek Epoch Microplate Spectrophotometer, Agilent) at a wavelength of 400 nm (Sancheti *et al.* 2009). The applied control was the enzyme reaction system devoid of SPLK. The percentage of inhibition was determined using the following equation:

$$\text{Inhibition (\%)} = \frac{\text{Control absorbance} - \text{Sample absorbance}}{\text{Control absorbance}} \times 100\%$$

2.4. Kinetics of Enzyme Inhibition

To determine the inhibition kinetics of SPLK against α-glucosidase, two reaction systems were used, including one without inhibition (substrate-enzyme) and the other featuring inhibition (substrate-enzyme-SPLK) (Sancheti *et al.* 2009). The velocity determination of enzyme reaction (v) was accomplished using the following formula:

$$v = \frac{[p\text{NP}]}{V \times t}$$

Where:

v : velocity of enzyme reaction (U/ml.minute)
[pNP] : concentration of p-nitrophenol formed (mM)
V : volume of enzyme in the reaction system (ml)
t : incubation duration (minutes)

The assessment of SPLK inhibition included the construction of a Lineweaver-Burk plot, plotting the x-axis with 1/[S] and the y-axis with 1/v. From this plot, the values of Michaelis Menten Constant (KM) and maximum velocity (v_{max}) were derived, while the Lineweaver-Burk equation is as follows:

$$\frac{1}{v} = \frac{K_M}{v_{max}} \cdot \frac{1}{[S]} + \frac{1}{v_{max}}$$

Where:

K_M : michaelis menten constant
v : velocity of enzyme reaction (U/ml.minute)
[S] : substrate concentration (mM)
v_{max} : maximum velocity of enzyme reaction (U/ml.minute)

2.5. Docking Analysis

A docking analysis was conducted to explore the inhibitory activity of SPLK against α-glucosidase through the *in silico* method. The 3D crystal structure of the enzyme was obtained from the Research Collaboratory for Structural Bioinformatics Protein Data Bank (https://www.rcsb.org) with PDB ID: 3TOP. The metabolites contained in *S. polyanthum* leaves and kombucha products were identified based on the literature review and applied as ligands in this analysis (Table 1). The 3D structure of the metabolites was sourced from the PubChem chemical database (https://pubchem.ncbi.nlm.nih.gov/). These selected metabolites adhered to Lipinski's rule for bioavailability, as determined using bioinformatics and computational biology web services

Table 1. Metabolites in *S. polyanthum* leaves and kombucha products

Metabolites	PubChem CID	Source	Structure	References
Malic acid	525	Leaves	$C_4H_6O_5$	Syabana *et al.* 2022
Gallic acid	370		$C_7H_6O_5$	
Protocatechuic acid	72		$C_7H_6O_4$	
Epigallocatechin gallate	65064		$C_{22}H_{18}O_{11}$	
Myricetin-3-O-rhamnoside	56843093		$C_{21}H_{20}O_{12}$	
Luteic acid	5319108		$C_{14}H_8O_9$	
Desmanthin-1	5316590		$C_{28}H_{24}O_{16}$	
Squalene	638072	Leaves	$C_{30}H_5O$	Widyawati *et al.* 2015
Nerolidol	5284507	Leaves	$C_{15}H_{26}O$	Rahim *et al.* 2018
Caryophyllene oxide	1742210		$C_{15}H_{24}O$	
Farnesol	445070		$C_{15}H_{26}O$	
Phytol	5280435		$C_{20}H_{40}O$	
Squalene	638072		$C_{30}H_5O$	
β-Tocopherol	6857447		$C_{28}H_{48}O_2$	
α-Tocopherol	14985		$C_{29}H_{50}O_2$	
β-Sitosterol	222284		$C_{29}H_{50}O$	
Acetic acid	176	Kombucha product	$C_2H_4O_2$	Leal *et al.* 2018
Glucuronic acid	94715		$C_6H_{10}O_7$	
D-saccharic acid 1,4 lactone	78997		$C_6H_8O_7$	
Glucuronic acid	94715	Kombucha product	$C_6H_{10}O_7$	Yang *et al.* 2022
Gluconic acid	10690		$C_6H_{12}O_0$	
Lactic acid	612		$C_3H_6O_3$	
Acetic acid	176		$C_2H_4O_2$	
Quercetin	5280343	Leaves	$C_{15}H_{10}O_7$	Dewijanti *et al.* 2020
Coniferin	5280372		$C_{16}H_{22}O_8$	
Juncusol	72740		$C_{18}H_{18}O_2$	
Retusin	5352005		$C_{19}H_{18}O_7$	
Hexadecanoic acid	985	Leaves	$C_{16}H_{32}O_2$	Widyawati *et al.* 2022
Octadecadienoic acid	5312457		$C_{18}H_{32}O_2$	
Stigmasterol	5280794		$C_{29}H_{48}O$	
Squalene	638072		$C_{30}H_{50}$	
Vitamin E	14985		$C_{29}H_{50}O_2$	
Valencene	9855795	Leaves	$C_{15}H_{24}$	Rochmat *et al.* 2022
α-Panasinsene	578929		$C_{15}H_{24}$	
Nerolidol	5284507		$C_{15}H_{26}O$	
Humulene Epoxide II	10704181		$C_{15}H_{24}O$	
α-Cubebene	86609		$C_{15}H_{24}$	
Azulene	9231		$C_{10}H_8$	
α-Pinene	6654		$C_{10}H_{16}$	
Cyclopropa naphthalene	15560278		$C_{15}H_{24}$	
Phytol	5280435		$C_{20}H_{40}O$	
Octadecatrienol	20295170		$C_{18}H_{32}O$	
Squalene	638072		$C_{30}H_{50}$	
α-Tocopherol	14985		$C_{29}H_{50}O_2$	
β-Sitosterol	222284		$C_{29}H_{50}O$	
Neophytadiene	10446		$C_{20}H_{38}$	

(http://www.scfbio-iitd.res.in/software/drugdesign/lipinski.jsp) (Jayaram *et al.* 2012).

The PyMOL Molecular Graphics System version 2.5.4 was deployed to separate ligand co-crystals, eliminate water molecules, and add hydrogen to macromolecules before docking. The ligand molecules were subjected to energy minimization using an MMFF94 force field to prevent interference during the docking simulation. This process was executed through Open Babel in PyRx software (PyRx-Phyton

Prescription 0.8) (Kudatarkar *et al.* 2021). Moreover, grid box settings were configured by positioning the X, Y, and Z coordinates at the center of amino acid residues (Thr1137, Glu1138, His1139, Pro1160, Gln1533, Lys1536, Ile1539, and Gly1540) initially predicted as allosteric sites with the Protein Allosteric Sites Server (PASSer) web service (https://passer.smu.edu) (Tian *et al.* 2023). The docking analysis was conducted with AutoDock Vina in PyRx software, then the results were evaluated and visualized using Discovery Studio Visualizer (BIOVIA Discovery Studio Visualizer V21.1.0.20298).

2.6. Protein and Small Molecules Network Analysis

The network analysis was performed to determine the interactions between the ligand molecules in this study and human proteins. The Search Tool for Interacting Chemicals (STITCH) web service (http://stitch.embl.de) was used for this purpose, with a high confidence interaction value set at 0.7 (Szklarczyk *et al.* 2016; Radhakrishnan *et al.* 2023).

3. Results

3.1. Phytochemical Components of SPLK

In this analysis, qualitative testing of phytochemical components was carried out. Flavonoid, saponin, and tannin tests showed positive results. Therefore, SPLK in this study does not contain terpenoids.

3.2. The pH Value of SPLK

The fermentation results showed variations in pH values from 2.86-3.09 (Figure 1). There is an inverse correlation between the pH value and sample concentration. The lowest pH value (2.86) was found at the highest sample concentration (50 g/L).

3.3. Inhibition of α-glucosidase

Each SPLK concentration had an inhibitory activity of 81.06-89.41% against α-glucosidase, showing a direct correlation between concentrations and inhibition activity (Figure 2). From the lowest sample concentration to a concentration of 37.5 g/L, the inhibitory activity was about 81.00-82.62% and increased significantly at the highest sample concentration. These results indicated the potential of SPLK as an α-glucosidase inhibitor.

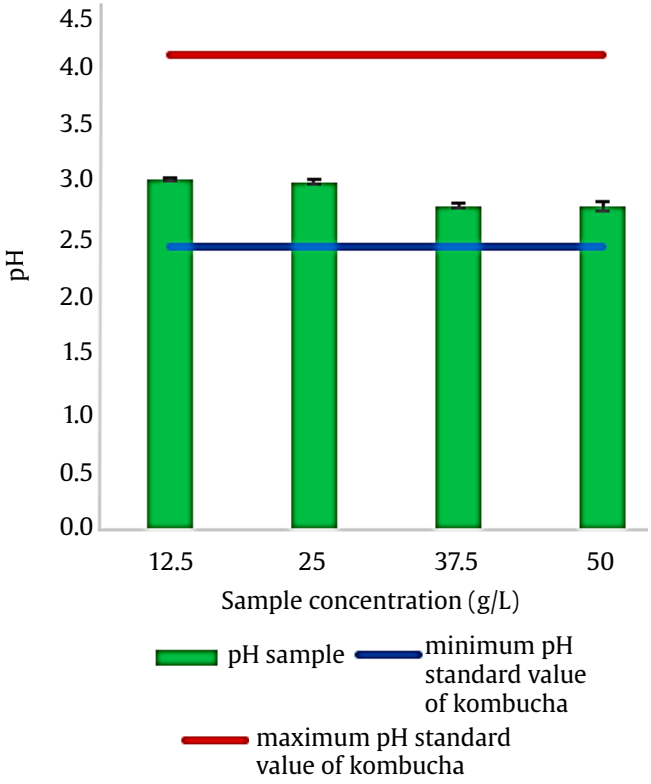

Figure 1. The pH value of *Syzygium polyanthum* (Wight) Walp. leaves kombucha at each concentration

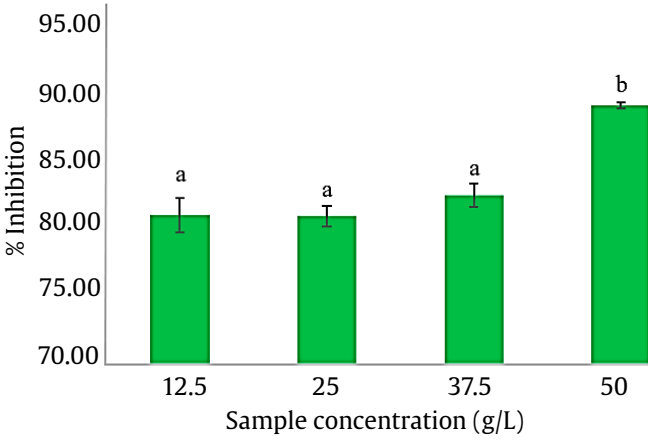

Figure 2. The inhibition activity of α-glucosidase from *Syzygium polyanthum* (Wight) Walp. Leave kombucha at each concentration. (Duncan test, $p<0.05$)

3.4. Kinetics of Enzyme Inhibition

In this study, the substrate concentration, known as pNPG, showed a direct correlation with α-glucosidase reaction rate since both parameters increased proportionally. The reaction rate in the absence of inhibitors had a higher value than when inhibitors (SPLK) were present due to α-glucosidase reacting more easily with the free form of pNPG (Figure 3). However, the reaction rate of α-glucosidase remained constant once saturated with pNPG because the substrate concentration had exceeded the enzyme reaction capacity after reaching the maximum velocity limit (v_{max}).

For enzyme kinetics calculation, The Michaelis-Menten equation was used to generate a Lineweaver-Burk plot, in which the K_M and v_{max} values were determined. The Lineweaver-Burk plot for the reaction without inhibitor, comprising enzyme and substrate, produced the equation y = 0.0155x + 0.0054, with v_{max} and K_M values of 185.1852 U/ml.minute and 2.9074 mM, respectively. The Lineweaver-Burk equation for the reaction system with inhibitor (SPLK) was y = 0.005x + 0.0361, with v_{max} of 27.708 U/ml.minute and K_M of 0.1357 mM (Figure 4). The v_{max} represented the maximum velocity of α-glucosidase in converting pNPG into products, including p-nitrophenol

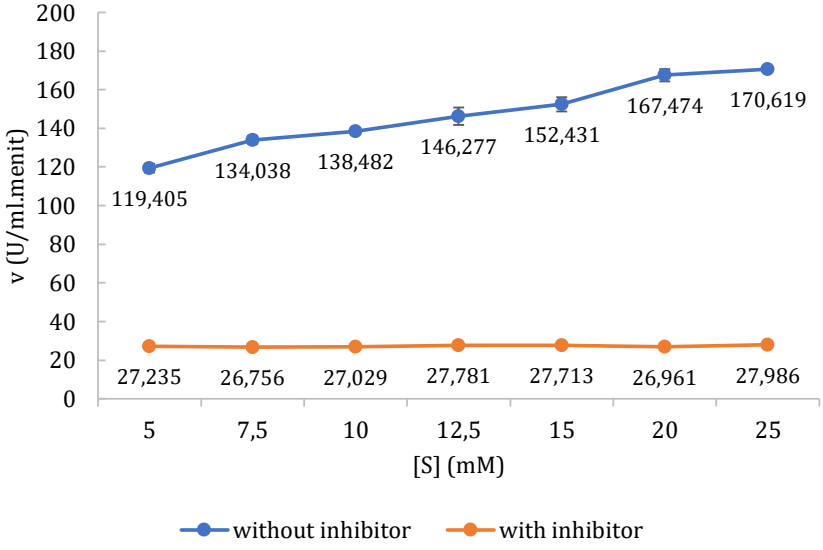

Figure 3. Correlation of α-glucosidase reaction velocity with various substrate concentrations. [S]: substrate concentration, v: velocity of enzyme reaction

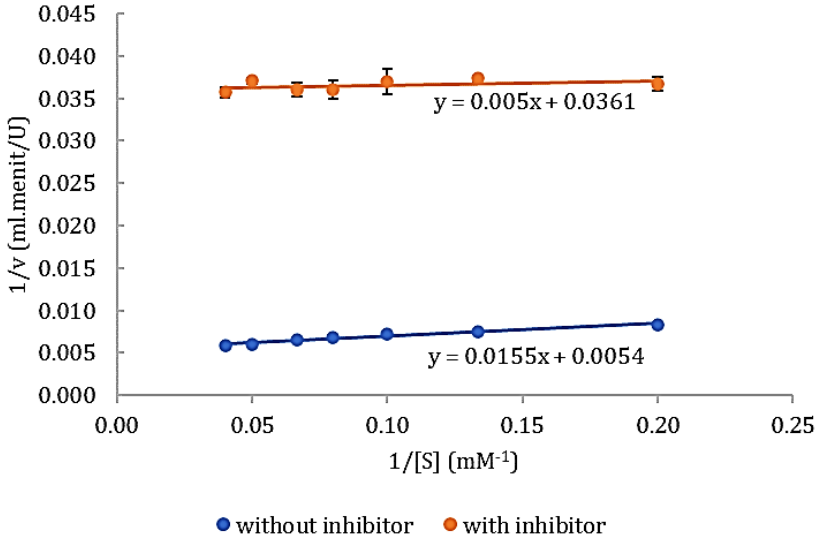

Figure 4. Lineweaver-Burk plot of α-glucosidase reaction. [S]: substrate concentration, v: velocity of enzyme reaction

and glucose, while the K_M showed the substrate concentration available when α-glucosidase reaction reached half of v_{max}. The K_M and v_{max} derived from the Lineweaver-Burk plot for the enzyme reaction without inhibitor were higher than their counterpart values. This observation showed that SPLK inhibited α-glucosidase activity through an uncompetitive inhibition mechanism.

3.5. Molecular Docking

In this analysis, the protein applied as a macromolecule was the A chain of human maltase glucoamylase (PDB ID: 3TOP). Additionally, the total ligands used included 12 metabolites evaluated based on Lipinski's rule, which helps to assess the drug-likeness of metabolites and predict their potential as drug-candidate compounds (Table 2). Based on the enzyme kinetics analysis in this study, SPLK was found to inhibit α-glucosidase through an uncompetitive mechanism. This type of inhibitor hinders product formation but does not obstruct substrate access to the catalytic site. During the analysis, the amino acid residue used as the coordinate center was the predicted allosteric site with the highest probability value. Meanwhile, the 3TOP protein contained a co-crystal ligand, acarbose, which was bound to the active site (Figure 5).

The test results showed six ligands with binding energies below -5.0 kcal/mol. These ligands included valencene, which had the lowest binding energy (-7.0 kcal/mol). Humulene epoxide II showed the highest binding energy (-0.5 kcal/mol) (Table 3). Each tested ligand showed hydrophobic and van der Waals interactions. Only farnesol shared an H-bond with Gln1533, and azulene was linked in an electrostatic π-anion interaction with Glu1138 (Figure 6).

3.6. Protein and SPLK Metabolite Network

The results of the molecular docking analysis showed that two of the six metabolites with the lowest binding energies (farnesol and α-pinene) have interacted with human proteins in the metabolic system. Farnesol was found to interact with caspase, reductase, transferase, and oxidase. Further, α-pinene has interaction with cytochrome P450 2B6 (Figure 7).

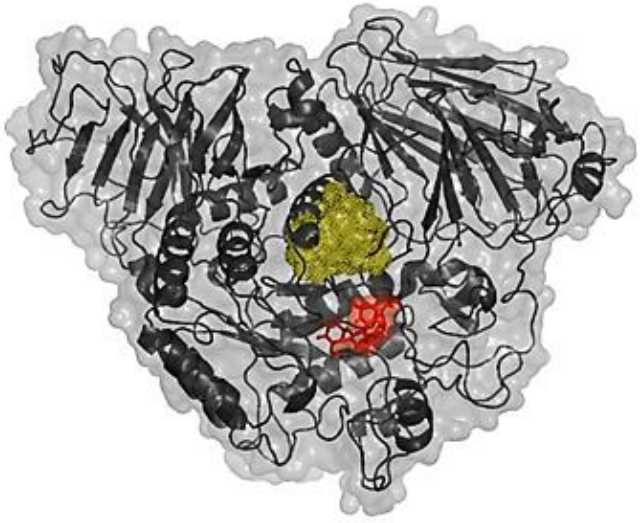

Figure 5. Protein structure (PDB ID: 3TOP) with acarbose in the active site (red) and the predicted allosteric site (yellow mesh)

Table 2. The metabolites used for molecular docking analysis were selected based on Lipinski's rules

Metabolites	Molecular weight	LogP	Hydrogen bond donors	Hydrogen bond acceptors	Molar refractivity
Nerolidol	222	4.396	1	1	72.47
Caryophyllene oxide	220	3.936	0	1	66.26
Farnesol	222	4.397	1	1	72.49
Juncusol	266	3.890	2	2	81.24
Retusin	358	3.008	1	7	93.09
Valencene	204	4.725	0	0	66.74
α-panasinsene	204	4.559	0	0	64.65
Humulune epoxide II	220	4.246	0	1	68.42
α-cubebene	204	4.270	0	0	64.51
Azulene	128	2.455	0	0	43.41
α-pinene	136	2.998	0	0	43.75
Cyclopropa naphthalene	204	4.441	0	0	64.58

Table 3. Docking analysis results of human maltase glucoamylase and selected metabolites

Metabolites	Binding energy (kcal/mol)	H-bond interacting residues	Hydrophobic bond interacting residues	van der Waals bond interacting residues	Electrostatic bond interacting residues
Valencene	-7.0		Pro1160, Tyr 1167, Leu1524, Lys1536, Ala1554	Glu1136, Thr1137, Glu1138, Ser1166, Gly1525, Asn1527, Gln1533, Ser1537, Gly1540, Glu1543, Phe1544	
Azulene	-5.9		Pro1160, Leu1524	Glu1136, Thr1137, Lys1536, Ser1537, Gly1540, Glu1543, Phe1544	Glu1138
α-cubebene	-5.8		Pro1160, Leu1524, Lys1536, Ala1554	Glu1136, Thr1137, Glu1138, His1139, Ser1166, Gly1525, Asn1527, Ser1537, Ile1539, Gly1540, Phe1544	
Farnesol	-5.7	Gln1533	Pro1160, Leu1524, Lys1536, Ile1539	Glu1136, Thr1137, Glu1138, His1139, Ser1166, Asn1527, Leu1534, Ser1537, Gly1540, Glu1543, Phe1544, Ala1554, Trp1571	
Nerolidol	-5.5		Pro1160, Leu1524, Lys1536, Ile1539, Ala1554, Trp1571	Glu1136, Thr1137, Glu1138, His1139, Ser1166, Asn1527, Ser1537, His1539, Gly1540, Glu1543, Phe1544,	
α-pinene	-5.5		Pro1160, Leu1524, Lys1536, Ile1539	Thr1137, Glu1138, His1139, Asn1527, Gln1533, Ser1537, Gly1540, Glu1543	

4. Discussion

Flavonoids, saponins, and tannins have been known to have inhibitory activity against α-glucosidase (Wang *et al.* 2010; Chukwujekwu *et al.* 2016; Lee *et al.* 2017). This scientific report supports the results obtained in this study. Additionally, these metabolites from kombucha showed antioxidant activity (Yuningtyas *et al.* 2021). Other constituents identified in 100 g of *S. polyanthum* leaves were 1 g protein, 12 g carbohydrates, 1 mg iron, 53 mg calcium, as well as trace amounts of potassium, vitamin A, and vitamin C (Spence 2023). In clinical trials, the fasting blood glucose level in patients with type 2 diabetes mellitus was decreased (8.85%) after 14 days *S. polyanthum* extract administration (Widyawati *et al.* 2019). Furthermore, the cookies containing 6% of *S. polyanthum* powder can reduce the glycemic response. In this case, consuming this cake does not significantly increase blood sugar levels (Khan *et al.* 2017). The substantial studies showed the *S. polyanthum* extract as an α-glucosidase inhibitor. This may result in reduced gastrointestinal glucose absorption (Widodo *et al.* 2023). We assume the mechanism for reducing blood glucose levels of *S. polyanthum* leaves as an α-glucosidase inhibitor.

The pH values of SPLK are within the standard pH range (2.5-4.2) for kombucha, according to The United

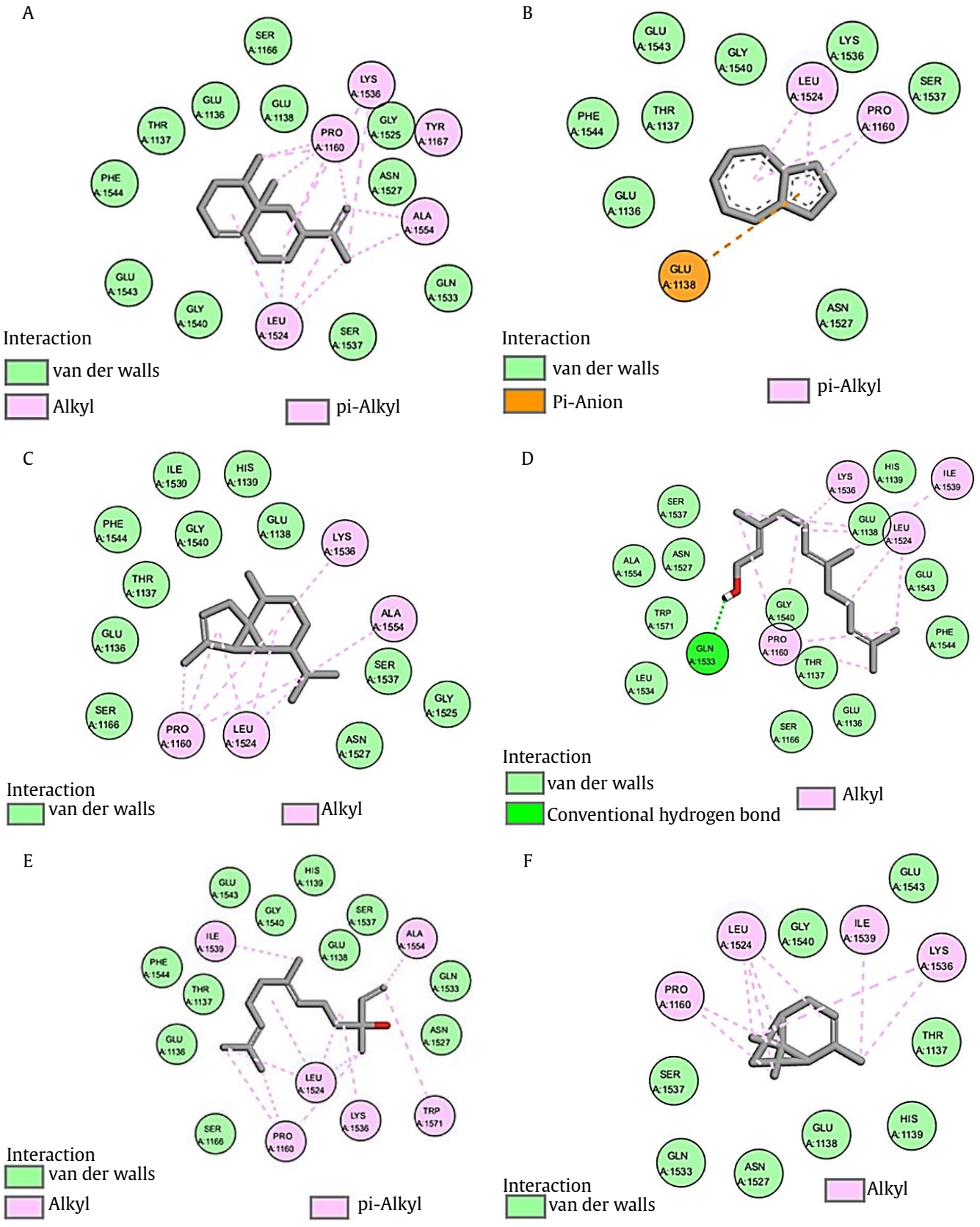

Figure 6. 2D ligand-protein interactions. (A) valencene, (B) azulene, (C) α-cubebene, (D) farnesol, (E) nerolidol, and (F) α-pinene

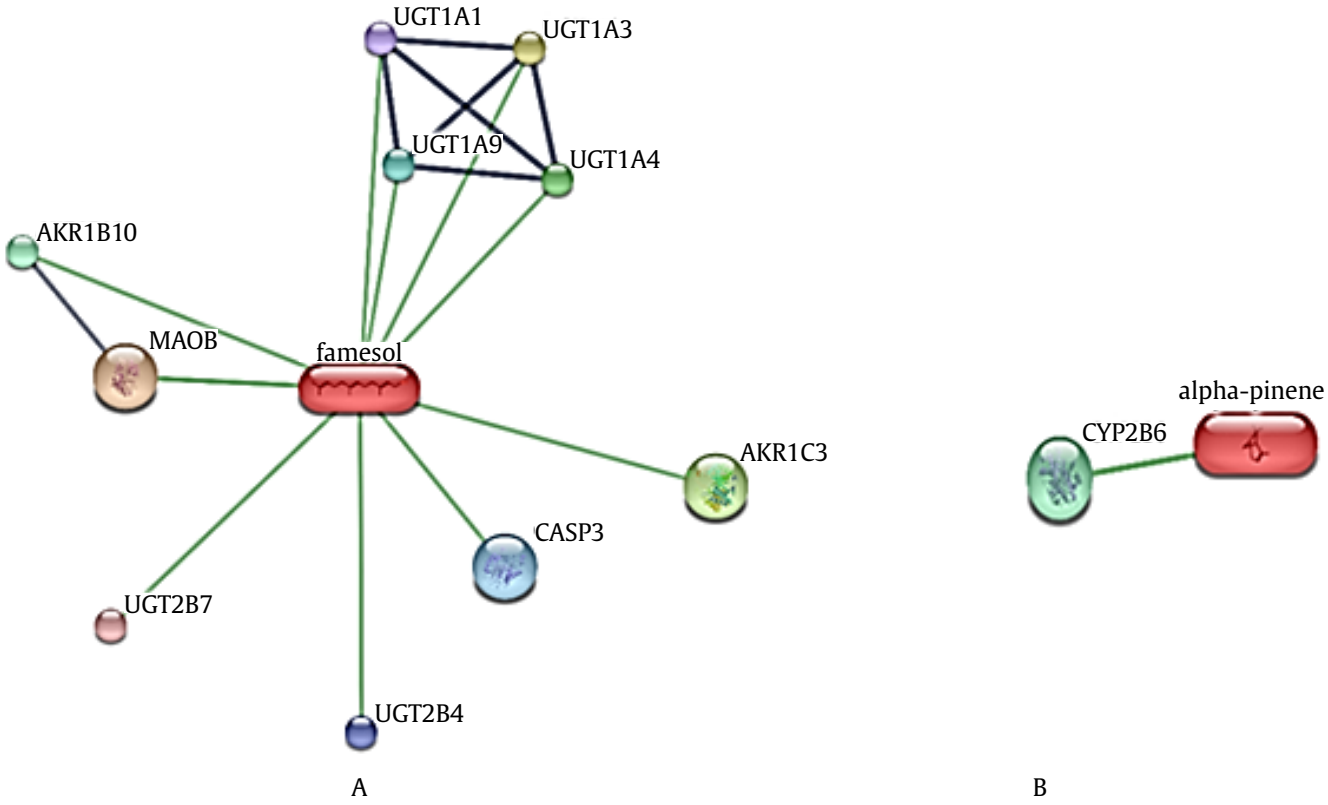

Figure 7. Human protein and SPLK metabolite network. (A) farnesol, (B) α-pinene. AKR1B10: aldo-keto reductase family 1, member B10; AKR1C3: aldo-keto reductase family 1, member C3; CASP3: caspase 3; MAOB: monoamine oxidase B; UGT1A1: UDP glucuronosyltransferase 1 family, polypeptide A1; UGT1A3: UDP glucuronosyltransferase 1 family, polypeptide A3; UGT1A4: UDP glucuronosyltransferase 1 family, polypeptide A4; UGT1A9: UDP glucuronosyltransferase 1 family, polypeptide A9; UGT2B4: UDP glucuronosyltransferase 2 family, polypeptide B4; UGT2B7: UDP glucuronosyltransferase 2 family, polypeptide B7; and CYP2B6: cytochrome P450, family 2, subfamily B, polypeptide 6

States Food and Drug Administration (Nummer 2013). The lower pH observed was a consequence of the organic acids generated during the fermentation process, increasing the total concentration of acidic compounds. The SCOBY used in kombucha production contained yeast capable of synthesizing the invertase enzyme, which cleaved the glycosidic bond in sucrose to yield glucose. Furthermore, glucose was oxidized into gluconolactone by glucose dehydrogenase. The gluconolactone was converted to gluconic acid by gluconolactone dehydrogenase. Since the fermentation process occurred anaerobically, glucose could be transformed into ethanol by yeast. The presence of *Acetobacter* sp. would facilitate the oxidation of ethanol to acetic and gluconic acids by alcohol dehydrogenase and aldehyde dehydrogenase. Additionally, the lactic acid bacteria component in the SCOBY contributed to the conversion of glucose into lactic acid (Laureys *et al.* 2020).

The composition of microorganisms in the SCOBY could influence SPLK characteristics, including the inhibitory effect exerted on the enzyme, due to the relationship between microorganism types present and the metabolites contained in the beverage (Jayabalan *et al.* 2014). Moreover, the fermentation process in SCOBY induced changes in organic acid and polyphenol levels, leading to more diverse organic acids, such as lactic, acetic, gluconic, and glucuronic acids, found in the obtained product (Jayabalan *et al.* 2017). *In vitro* inhibition of α-glucosidase by SPLK signified its potential as an antidiabetic agent. However, α-glucosidase inside the small intestine plays a crucial role in hydrolyzing α-1,4 glycoside bonds in polysaccharides to synthesize monosaccharides, specifically glucose, which can be easily absorbed. Inhibition of this enzyme would disrupt the hydrolysis process, inhibiting both absorption and the increase in blood glucose

levels. This mechanism appeared to be effective in preventing the occurrence of hyperglycemia. Therefore, *in vitro* assessment conducted using natural ingredients such as SPLK provided a basis for evaluating their antidiabetic potential (Lankatillake *et al.* 2019).

Enzyme kinetics parameters, including K_M and v_{max}, are essential for understanding enzyme action mechanisms and metabolic role, as well as the mechanisms of enzyme-inhibiting drugs (Rodríguez *et al.* 2022). In the uncompetitive inhibition mechanism, despite the enzyme-substrate complex (ES) has been formed, the allosteric site of the enzyme can still bind the inhibitor to form an enzyme-substrate-inhibitor complex (ES-I). ES complexes bound to uncompetitive inhibitors are mostly formed under conditions of high substrate concentration, and products cannot be generated from the ES-I complex once inhibitors are bound, leading to a decrease in the vmax value. Product synthesis resumes upon inhibitor dissociation from the complex (Nelson and Cox 2008).

Lipinski's rule was used for characterizing metabolites physicochemical. These characteristics are important to determine the level of permeability of drug candidate compounds. This rule states that metabolites with good drug-like properties have molecular masses below 500 Da, high lipophilicity (expressed as LogP values > 5), > 5 hydrogen bond donors, >10 hydrogen bond acceptors, and molar refractivity values ranging from 40-130 (Lipinski 2004).

We used the PASSer web service for allosteric site prediction with AutoML prediction criteria. Identifying allosteric sites is essential for understanding the biological process (Tian *et al.* 2023). The uncompetitive inhibitor has a different binding site from the active site, with the result necessary to identify the inhibition binding site (Sakulkeo *et al.* 2022). The prediction result showed a different site between the active site and the allosteric site (inhibitor binding site) (Figure 5). The active site of 3TOP protein has co-crystal ligand with H-bonds (Arg1510, Asp1526, His1584, Asp1157, and Asp1279) and hydrophobic interactions (Tyr1251, Ile1280, Trp1355, Trp1418, Asp1420, Met1421, Trp1523, and Phe1559) (Ren *et al.* 2011).

The binding energy and types of molecular interactions are used to analyze protein and ligand interactions. The lowest binding energy possessed by a ligand shows its potential as an inhibitor in an enzyme inhibition reaction (Ramos *et al.* 2021). H-bond interactions featured lower energy than covalent bonds but appeared stronger than van der Waals forces, playing a crucial role in biochemical processes such as enzyme catalysis. Conventionally, these bonds form between N-H...O and O-H...O (Bulusu and Desiraju 2019). Hydrophobic interactions occur between nonpolar molecules in a polar solvent (water) and are essential for stabilizing protein structures (Bogunia and Makowski 2020). Amino acid residues Pro1160 and Leu1524 consistently participated in hydrophobic interactions with all ligands tested in this study (Figure 6). This phenomenon could be attributed to both amino acids belonging to the aliphatic hydrophobic group and facilitating the stabilization of secondary, tertiary, and quaternary protein structures through hydrophobic interactions (Mughram *et al.* 2023). Furthermore, van der Waals interactions in the conducted analysis constituted many amino acid residues. They were formed from transient dipole moments existing in atoms or molecules, leading to weak interactions between molecules with opposite transient charges. The strength of this interaction decreased as the distance between the two molecules increased (Singh 2016). The presence of a π-anion interaction in the aromatic ring of azulene is facilitated by the acidic side chain of a Glu138 residue bonding as anions with the azulene ring (Borozan *et al.* 2016) (Figure 6B).

The role of small molecules with other molecules, such as proteins, in biological processes needs to be understood for drug development. Farnesol and α-pinene have interactions with human enzymes. Farnesol has been reported to induce apoptosis in human oral squamous carcinoma and meningioma cells by enhancing caspase-3 activity (Jung *et al.* 2018). In the metabolism process, farnesol could be oxidized to become farnesal and subsequently converted into farnesoic acid. The rate of catabolism for synthesizing farnesoic acid in MCF-7 cells was discovered to be influenced by human aldo-keto reductase (AKR1C3), determining the bioavailability of farnesol (Endo *et al.* 2011). Farnesol could be metabolized to farnesyl glucuronide, hydroxyfarnesol, and hydroxyfarnesyl glucuronide by enzymes from the uridine diphosphoglucuronosyltransferases (UGTs) family (Staines *et al.* 2004). Additionally, the competitive

inhibition of farnesol with human monoamine oxidase B (drugs target for neurological disorders) signifies the promising application for neurological health treatment (Binda *et al.* 2002; Hubálek *et al.* 2005). Furthermore, α-pinene is an inhibitor of cytochrome P450 2B6. This interaction occurs in the active site of the enzyme (Wilderman *et al.* 2013).

In conclusion, SPLK showed significant potential as a health-promoting beverage due to its content of flavonoids, saponins, and tannins, with beneficial bioactivities. This product was identified as an uncompetitive inhibitor of α-glucosidase through enzymatic reaction and *in silico* studies, making it a promising alternative therapy for diabetic patients. However, these observations necessitated further validation through analytical methods using experimental animals. The protein and small molecule network analysis showed the applicability of SPLK for developing functional beverages targeting various diseases. However, further investigations should be conducted to confirm this potential.

Acknowledgements

The authors are grateful to Herson Cahaya Himawan for facilitating this study and providing valuable suggestions to improve the manuscript.

References

Binda, C., Vinson, P.N., Hubálek, F., Edmondson, D.E., Mattevi, A., 2002. Structure of human monoamine oxidase B, a drug target for the treatment of neurological disorders. *Nat. Struct. Biol.* 9, 22–26. https://doi.org/10.1038/nsb732

Bogunia, M., Makowski, M., 2020. Influence of ionic strength on hydrophobic interactions in water: dependence on solute size and shape. *J. Phys. Chem. B.* 124, 10326–10336. https://doi.org/10.1021/acs.jpcb.0c06399

Borozan, S.Z., Zlatović, M.V., Stojanović, S.D., 2016. Anion–π interactions in complexes of proteins and halogen-containing amino acids. *Biol. Inorg. Chem.* 21, 357–368. https://doi.org/10.1007/s00775-016-1346-y

Bulusu, G., Desiraju, G.R., 2019. Strong and weak hydrogen bonds in protein-ligand recognition. *J. Indian Inst. Sci*. 100, 31-41. https://doi.org/10.1007/s41745-019-00141-9

Chukwujekwu, J.C., Rengasamy, K.R.R., Kock, C.A.D., Smith, P.J., Slavětínská, L.P., Staden, J.V., 2016. Alpha-glucosidase inhibitory and antiplasmodial properties of terpenoids from the leaves of *Buddleja saligna* Willd. *J. Enzyme Inhibition Med. Chem.* 31, 63-66. https://doi.org/10.3109/14756366.2014.1003927

Dewijanti, I.D., Mangunwardoyo, W., Dwiranti, A., Hanafi, M., Artanti, N., 2020. Effects of the various source areas of Indonesian bay leaves (*Syzygium polyanthum*) on chemical content and antidiabetic activity. *Biodiversitas.* 21, 1190-1195. https://doi.org/10.13057/biodiv/d210345

Dutta, H., Paul, S.K., 2019. 8-Kombucha drink: production, quality, and safety aspects, production and management of beverages, in: Alexandru Mihai Grumezescu, Alina Maria Holban (Eds.), *Production and Management of Beverages*. Elsevier Inc., Duxford, pp. 259-288. https://doi.org/10.1016/B978-0-12-815260-7.00008-0

Endo, S., Matsunaga, T., Ohta, C., Soda, M., Kanamori, A., Kitade, Y., Ohno, S., Tajima, K., El-Kabbani, O., Hara, A., 2011. Roles of rat and human aldo–keto reductases in metabolism of farnesol and geranylgeraniol. *Chemico-Biological Interactions.* 191, 261–268. https://doi.org/10.1016/j.cbi.2010.12.017

Hubálek, F., Binda, C., Khalil, A., Li, M., Mattevi, A., Castagnoli, N., Edmondson, D.E., 2005. Demonstration of isoleucine 199 as a structural determinant for the selective inhibition of human monoamine oxidase B by specific reversible inhibitors. *J. Biol. Chem.* 280, 15761–15766. https://doi.org/10.1074/jbc.M500949200

Ismail, A., Ahmad, W.A.N.W., 2019. *Syzygium polyanthum* (Wight) Walp: a potential phytomedicine. *Pharmacogn. J.* 11, 429-438. https://doi.org/10.5530/pj.2019.11.67

Jayabalan, R., Malbaša, R.V., Lončar, E.S., Vitas, J.S., Sathishkumar, M., 2014. A Review on kombucha tea—microbiology, composition, fermentation, beneficial effects, toxicity, and tea fungus. *Comprehensive Rev. Food Sci. Food Safety*. 13, 538-550. https://doi.org/10.1111/1541-4337.12073

Jayabalan, R., Malbaša, R.V., Sathishkumar, M., 2017. Kombucha tea: metabolites, in: Mérillon, J.M.., Ramawat, K., (Eds.), *Fungal Metabolites, Reference Series in Phytochemistry*. Springer, Cham, pp. 965-978. https://doi.org/10.1007/978-3-319-25001-4_12

Jayaram, B., Singh, T., Mukherjee, G., Mathur, A., Shekhar, S., Shekhar, V., 2012. Sanjeevini: a freely accessible web-server for target directed lead molecule discovery. *BMC Bioinformatics* 13, S7. https://doi.org/10.1186/1471-2105-13-S17-S7

Jung, Y.Y., Hwang, S.T., Sethi, G., Fan, L., Arfuso, F., Ahn, K.S., 2018. Potential anti-inflamatory and anti-cancer properties of farnesol. *Molecules.* 23, 2827. https://doi.org/10.3390/molecules23112827

Kementerian Kesehatan Republik Indonesia. 2020. *Pusat Data dan Informasi Kementerian Kesehatan RI: Tetap Produktif, Cegah, dan Atasi Diabetes Melitus*. Kemenkes RI, Jakarta.

Khan I, Shah S, Ahmad J, Abdullah A, Johnson SK. 2017. Effect of incorporating bay leaves in cookies on postprandial glycemia, appetite, palatability, and gastrointestinal well-being. *J. Am. Coll. Nutr.* 36, 514-517. https://doi.org/10.1080/07315724.2017.1326324

Kudatarkar, N., Jalalpure, S., Patil, V.S., Kurangi, B., 2021. System biology and chemoinformatics approaches to decode the molecular mechanisms of chrysin against colon cancer. *J. Appl. Pharm. Sci.* 11, 57-65. https://doi.org/10.7324/JAPS.2021.110907

Lankatillake, C., Huynh, T., Dias, D.A., 2019. Understanding glycaemic control and current approaches for screening antidiabetic natural products from evidence-based medicinal plants. *Plant Methods.* 15, 105. https://doi.org/10.1186/s13007-019-0487-8

Laureys, D., Britton, S.J., Clippeleer, J.D., 2020 Kombucha tea fermentation: a review. *J. Am. Soc. Brewing Chemists.* 78, 165-174. https://doi.org/10.1080/03610470.2020.1734150

Leal, J.M., Suárez, L.V., Jayabalan, R., Oros, J.H., Aburto, A.E., 2018. A review on health benefits of kombucha nutritional compounds and metabolites. CyTA-*Journal of Food.* 16, 390-399. https://doi.org/10.1080/19476337.2017.1410499

Lee, D.Y., Kim, H.W., Yang, H., Sung, S.H., 2017. Hydrolyzable tannins from the fruits of *Terminalia chebula* Retz and their α-glucosidase inhibitory activities. *Phytochem.* 137, 109–116. https://doi.org/10.1016/j.phytochem.2017.02.006

Lipinksi, C.A., 2004. Lead and drug like compounds: the rule of five revolution. *Drug Discovery Today: Tehcnologies.* 1, 337-341. https://doi.org/10.1016/j.ddtec.2004.11.007

Mughram, M.H.A., Catalano, C., Herrington, N.B., Safo, M.K., Kellogg, G.E., 2023. 3D interaction homology: the hydrophobic residues alanine, isoleucine, leucine, proline and valine play different structural roles in soluble and membrane proteins. *Front Mol. Biosci.* 10, 1116868. https://doi.org/10.3389/fmolb.2023.1116868

Nelson, D.L., Cox, M.M., 2008. *Lehninger: Principles of Biochemistry,* fifth ed. WH Freeman and Company, New York.

Nummer, B.A., 2013. Kombucha brewing under The Food and Drug Administration (FDA) model food code: risk analysis and processing guidance. *J. Environ. Health* 76, 8-11.

Radhakrishnan, N., Prabhakaran, V.S., Wadaan, M.A., Baabbad, A., Vinayagam, R., Kang, S.G., 2023. STITCH, physicochemical, ADMET, and *in silico* analysis of selected Mikania constituents as anti-inflammatory agents. *Processes.* 11, 1722. https://doi.org/10.3390/pr11061722

Rahim, E.N.A.A., Ismail, A., Omar, M.N., Rahmat, U.N., Ahmad, W.A.N.W., 2018. GC-MS analysis of phytochemical compounds in *Syzygium polyanthum* leaves extracted using ultrasound-assisted method. *Pharmacogn. J.* 10, 110-119. https://doi.org/10.5530/pj.2018.1.20

Ramos, D.R., Magallanes, B.O., Espinosa, J.F.P., Rubalcava, M.L.M., Raja, H.A., Andrade, M.G., Mata, R., 2021. α-glucosidase and PTP-1B inhibitors from Malbranchea dendritica. *ACS Omega.* 6, 22969–22981. https://doi.org/10.1021/acsomega.1c03708

Ren, L., Qin, X., Cao, X., Wang, L., Bai, F., Bai, G., Shen, Y., 2011. Structural insight into substrate specificity of human intestinal maltase-glucoamylase. *Protein Cell.* 2, 827-836. https://doi.org/10.1007/s13238-011-1105-3

Rochmat, A., Aditya, G., Kusmayanti, N., Kustiningsih, I., Hariri, A., Rezaldi, F., 2022. *In vitro* activity and docking approach in silico leaf extract *Syzygium polyanthum* (Wight) Walp. as a *Salmonella typhi* inhibitor. *Trends Sci.* 19, 5654. https://doi.org/10.48048/tis.2022.5654

Rodríguez, J.A.P., Mena, K.P.L., Muñoz, J.C.C., Amin, J.E.P., Vallejo, F.L., Suárez, L.E.C., Ladino, O.J.P., 2022. *In vitro* and *in silico* study of the α-glucosidase and lipase inhibitory activities of chemical constituents from *Piper cumanense* (Piperaceae) and synthetic analogs. *Plants.* 11, 2188. https://doi.org/10.3390/plants11172188

Sakulkeo, O., Wattanapiromsakul, C., Pitakbut, T., Dej-adisai, S., 2022. Alpha-glucosidase inhibition and molecular docking of isolated compounds from traditional Thai medicinal plant, *Neuropeltis racemosa* Wall. *Molecules.* 27, 639. https://doi.org/10.3390/molecules27030639

Sancheti, S., Sancheti, S., Seo, S.Y., 2009. Chaenomeles sinensis: a potent α-and β-glucosidase inhibitor. *Am. J. Pharmacol. Toxicol.* 4, 8–11. https://doi.org/10.3844/ajptsp.2009.8.11

Singh, A.K., 2016. Chapter 8 nanoparticle ecotoxicology. in: Ashok, K. Singh (Eds.), *Engineered Nanoparticles.* Academic Press, San Diego, pp. 343-450. https://doi.org/10.1016/B978-0-12-801406-6.00008-X

Sivanandham, V., 2015. Phytochemical techniques - a review. *World J. Sci Res.* 1, 80–91.

Spence, C., 2023. Why cook with bay leaves?. *Int. J. Gastronomy Food Sci.* 33, 100766. https://doi.org/10.1016/j.ijgfs.2023.100766

Staines, A.G., Sindelar, P., Coughtrie, M.W.H., Burchell, B., 2004. Farnesol is glucuronidated in human liver, kidney and intestine in vitro, and is a novel substrate for UGT2B7 and UGT1A1. *Biochem.* 384, 637–645. https://doi.org/10.1042/BJ20040997

Syabana, M.A., Yuliana, N.D., Batubara, I., Fardiaz, D., 2022. α-glucosidase inhibitors from *Syzygium polyanthum* (Wight) Walp leaves as revealed by metabolomics and *in silico* approaches. *J. Ethnopharmacol.* 282, 114618. https://doi.org/10.1016/j.jep.2021.114618

Szklarczyk, D., Santos, A., Mering, C.V., Jensen, L.J., Bork, P., Kuhn, M., 2016. STITCH 5: augmenting protein–chemical interaction networks with tissue and affinity data. *Nucleic Acids Res.* 44, 380–384. https://doi.org/10.1093/nar/gkv1277

Tian, H., Xiao, S., Jiang, X., Tao, P., 2023. PASSer: fast and accurate prediction of protein allosteric sites. *Nucleic Acids Res.* 51, 427-431. https://doi.org/10.1093/nar/gkad303

Wahjuni, S., Laksmiwati, A.A.I.A.M., Manuaba, I.B.P., 2018. Antidiabetic effects of Indonesian bay leaves (*Syzygium polyanthum*) extracts through decreasing advanced glycation end products and blood glucose level on alloxan-induced hyperglycemic wistar rats. *Asian J. Pharm. Clin. Res.* 11, 340-343. https://doi.org/10.22159/ajpcr.2018.v11i4.24084

Wang, H., Du, Y.J., Song, H.C., 2010. α-glucosidase and α-amylase inhibitory activities of guava leaves. *Food. Chem.* 123, 6–13. https://doi.org/10.1016/j.foodchem.2010.03.088.

Widodo, W.D.P., Parisa, N., Tamzil, N.S., Lusiana, E., Ardita, N., Putri, A.A.A., Permata, S.B., Ditamor, A.F., 2023. The potential of bay leave (*Syzygium polyanthum*) as an anti-diabetic agent. *IJICM.* 4, 63-70. https://doi.org/10.55116/IJICM.V4I2.60.

Widyawati, T., Yusoff, N.A., Asmawi, M.Z., Ahmad, M., 2015. Antihyperglycemic effect of methanol extract of *Syzygium polyanthum* (Wight.) leaf in streptozotocin-induced diabetic rats. *Nutrients.* 7, 7764-7780. https://doi.org/10.3390/nu7095365

Widyawati, T., Pase, N.A., Daulay, M., Sumantri, I.B., 2019. Effect of bay leaf ethanol extract on blood glucose level in Patients with type 2 diabetes mellitus. *In: The 6th International Conference on Public Health.* Surakarta: Universitas Sebelas Maret. pp. 613-617. https://doi.org/10.26911/the6thicph-FP.05.07

Widyawati, T., Yusoff, N.A., Bello, I., Asmawi, M.Z., Ahmad, M., 2022. Bioactivity-guided fractionation and identification of antidiabetic compound of *Syzygium polyanthum* (Wight.)'s leaf extract in streptozotocin-Induced diabetic rat model. *Molecules.* 27, 6814. https://doi.org/10.3390/molecules27206814

Wilderman, P.R., Shah, M.B., Jang, H.H., Stout, D., Halpert, J.R., 2013. Structural and thermodynamic basis of (+)-α-pinene binding to human cytochrome P450 2B6. *J. Am. Chem. Soc.* 135, 10433–10440. https://doi.org/10.1021/ja403042k

Yang, J., Lagishetty, V., Kurnia, P., Henning, S.M., Ahdoot, A.I., Jacobs, J.P., 2022. Microbial and chemical profiles of commercial kombucha products. *Nutrients.* 14, 670. https://doi.org/10.3390/nu14030670

Yuningtyas, S., Masaenah, E., Telaumbanua, M., 2021. Aktivitas antioksidan, total fenol, dan kadar vitamin C dari kombucha daun salam (*Syzygium polyanthum* (Wight) Walp). *Pharmamedica J.* 6, 10–14. https://doi.org/10.47219/ath.v6i1.116